ChemComm

SUPPORTING INFORMATION

Photocatalytic hydrogen evolution on Si photocathodes modified with bis(thiosemicarbazonato)nickel(II)/Nafion

Saumya Gulati,[a] Oleksandr Hietsoi,[b] Caleb A. Calvary,[b] Jacob M. Strain,[a] Sahar Pishgar,[a] Henry C. Brun,[b] Craig A. Grapperhaus,[b] Robert M. Buchanan,*[b] and Joshua M. Spurgeon*[a]

Experimental Methods

NiATSM Catalyst Synthesis and Characterization

All reagents were obtained from commercially available sources and used as received unless otherwise noted. Commercial solvents were additionally dried and purified using an MBraun solvent purification system unless otherwise noted. All reactions were performed open to air and under ambient conditions unless otherwise indicated. The diacetyl-bis(N-4-methyl-3-thiosemicarbazone) (H_2ATSM) ligand and the diacetyl-bis(N-4-methyl-3-thiosemicarazonato)nickel(II) (NiATSM) complex were prepared following previously reported methods.[1, 2]

The prepared NiATSM complex was characterized by NMR (Fig. 1), elemental analysis, FT-IR (Fig. S1), and UV/vis spectroscopy (Fig. S2). The ^{1}H NMR data were collected on a Varian *Inova* 500 MHz NMR Spectrometer in commercial deuterated solvents (Aldrich or Cambridge Isotopes). The ^{1}H NMR of NiATSM displays characteristic peaks at 1.94 ppm for the backbone methyl protons, at 2.75 ppm for the pendant methyl protons, and at 7.69 ppm for the pendant NH protons (Fig. 1). Elemental analyses were performed by Midwest Microlab, (Indianapolis, IN, USA). The purity of NiATSM complex was confirmed by elemental analysis: Anal. Calc. for $C_8H_{14}N_6NiS_2$: C, 30.31; H, 4.45; N, 26.51. Found: C, 30.55; H, 4.35; N, 26.42. Infrared spectra were recorded on a Thermo Nicolet Avatar 360 spectrometer equipped with an ATR attachment (4 cm^{-1} resolution). The infrared spectrum of the H_2ATSM ligand displays two N–H stretches at 3238 and 3357 cm^{-1}. Upon complexation of H_2ATSM with Ni(II) the characteristic hydrazino N–H stretch at 3238 cm^{-1} disappears in the NiATSM spectrum (Fig. S1). Electronic UV/vis absorption spectra were recorded with an Agilent 8453 diode array spectrometer with a 1 cm path length quartz cell. The electronic spectrum of H_2ATSM displays a strong band at 328 nm that upon complexation with Ni(II) is significantly decreased with the appearance of a ligand-to-metal charge-transfer band near 398 nm and a more intense ligand-to-ligand charge-transfer band near 257 nm in the NiATSM spectrum (Fig. S2).

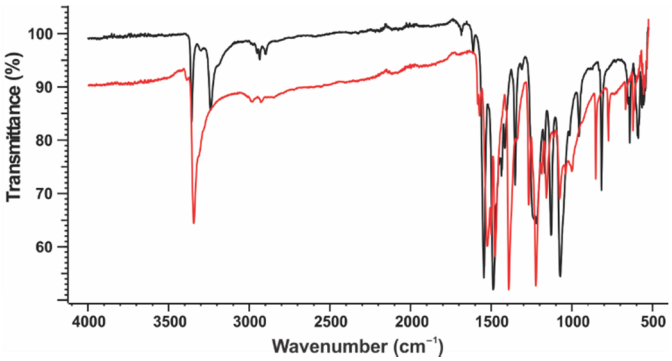

Fig. S1. FT-IR spectra of H_2ATSM (black) and NiATSM (red).

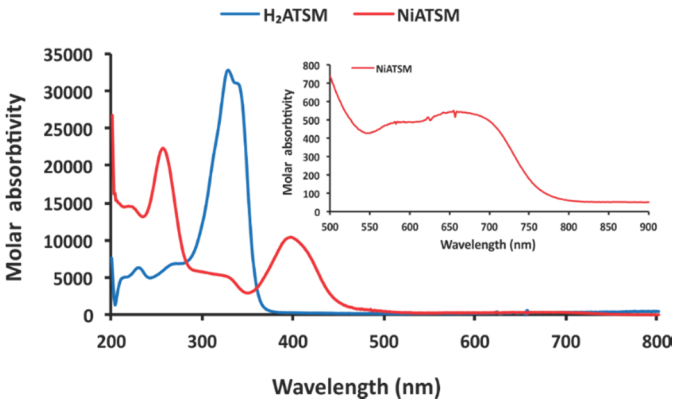

Fig. S2. UV-vis spectra of H_2ATSM (blue) and NiATSM (red) recorded in a mixture of acetonitrile/methanol solution (1:1). (Inset) The d-d charge-transfer region.

Electrode Preparation

Two different types of Si substrate were used in this work. Degenerately doped n$^+$-Si(100) (doped with As to a resistivity of 0.001 – 0.005 Ω cm, University Wafer) substrates were used to measure the dark electrocatalytic behavior of the Si semiconductor surface as well as the Si-supported NiATSM electrocatalyst behavior. Photoactive substrates for illuminated hydrogen evolution consisted of p-Si(100) (doped with B to 1 – 10 Ω cm, University Wafer). Before attaching the NiATSM co-catalyst, the Si native oxide layer was removed with a > 10 s dip in 10% HF. To load the catalyst on the electrodes, a 2.0 mM

[a] Conn Center for Renewable Energy Research, University of Louisville, Louisville, Kentucky, 40292, USA. E-mail: joshua.spurgeon@louisville.edu
[b] Department of Chemistry, University of Louisville, 2320 South Brook Street, Louisville, Kentucky 40292, USA. E-mail: robert.buchanan@louisville.edu

solution of NiATSM in acetonitrile was dropcast on the Si surface to a consistent loading of ~60 nmol cm^{-2}, followed by 1 min in a vacuum oven at 70 °C. For Nafion-bound NiATSM, each 20 mL of 2 mM solution also contained 25 µL of 5% aqueous Nafion solution (Beantown Chemical) and was further heated in air at 60 °C for 1 min. In the case of electrodeposited Ni metal catalyst on p-Si for comparison, the Si working electrode was placed in nickel electroplating solution (nickel sulfamate and boric acid, Sigma Aldrich) with a Ag/AgCl reference and a fritted Pt counter electrode and held at -0.5 V vs. RHE under illumination to pass various amounts of charge corresponding to different Ni loadings. To match the molar loading of Ni atoms on the NiATSM/p-Si electrodes with 60 nmol NiATSM cm^{-2}, a charge of 0.012 C cm^{-2} was passed. An ohmic back contact to Si substrates was made using Ga/In eutectic (Alfa Aesar), with the back contact sealed in epoxy. Pt deposition on p-Si was accomplished via a galvanic displacement reaction whereby Si is oxidized (and then etched by HF) and Pt is reduced onto the electrode surface.[3] The Si wafer was immersed for 2 minutes in an aqueous solution of 0.5 M HF and 2 mM K_2PtCl_6.[4] The n^+ p junction was formed on the Si by thermal P diffusion using solid-source CeP_5O_{14} wafers (Saint-Gobain, PH-900 PDS) at 950 °C for 30 min under N_2 ambient, to yield an n^+ emitter layer. The room temperature n^+p-Si was then etched in 10% HF for > 2 min to remove the dopant glass layer, followed by physical abrasion of the wafer edges to eliminate shunting.

Photoelectrochemical Measurements

Current density vs. potential (*J-E*) photoelectrochemical energy-conversion behavior for all electrodes was measured in hydrogen-saturated 1 M H_2SO_4 (pH 0, made with 18 MΩ cm H_2O) under vigorous stirring with active bubbling of H_2 (99.99%, Specialty Gases) at room temperature. The Si electrode was the working electrode in each case, with a Ag/AgCl (saturated KCl) reference electrode (CH instruments, Inc.) along with a Pt gauze counter electrode separated by a glass frit, all in a glass cell with a flat quartz window for illumination. Before each measurement with a Si electrode, the native oxide was removed with a > 10 s dip in 10% HF. A Bio-Logic SP-200 potentiostat was used for all measurements. The results are reported versus the reversible hydrogen electrode (RHE) scale according to $V_{RHE} = V_{Ag/AgCl} + 0.197 + 0.059*pH$. Simulated sunlight at an intensity of 100 mW cm^{-2} at normal incidence to the working electrode was generated with a 300 W Xe lamp (Newport 6258) coupled with an AM1.5 global filter (Newport 81094) and calibrated in the electrolyte with a Si photodiode (Thorlabs FDS100-CAL). Cyclic voltammetry measurements of *J-E* behavior were measured at a scan rate of 20 mV s^{-1}. Reported 1 h stability data was measured potentiostatically at -0.2 V vs. RHE.

Hydrogen quantification and faradaic efficiency determination were measured under potentiostatic conditions at -0.2 V vs. RHE using gas chromatography (GC, SRI 8610). For this measurement, H_2 was not bubbled but instead nitrogen (99.99%, Specialty Gases) was used as the carrier gas to enable accurate hydrogen quantification. The gas outlet from the catholyte was connected to the GC, which used an automatic valve injection (1 mL sample) and a thermal conductivity detector (TCD). Faradaic efficiency was calculated by determining the charge required to produce the measured H_2 concentration and dividing by the total charge passed in the electrolysis during the gas collection period.

Materials Characterization

The electrode surfaces were characterized with scanning electron microscopy (SEM) using a NOVA FEI microscope at an accelerating voltage of ~ 15 – 18 kV. Energy dispersive X-ray spectroscopy (EDS) mapping measurements were conducted using an FEI Tecnai F20 microscope with an accelerating voltage of 20 kV. Surface elemental analysis was performed using X-ray photoelectron spectroscopy (XPS) with a VG Scientific Multilab 3000 custom-built ultra-high vacuum system with Mg-Kα radiation. XPSPEAK 4.1 software was used for peak deconvolution and the XPS data analysis.

Nafion Binding Effect on *J-E* Behavior Stability

Although the *J-E* behavior of drop-cast NiATSM on p-Si initially showed a significant positive shift in the potential relative to bare p-Si, this enhancement was not stable under extended

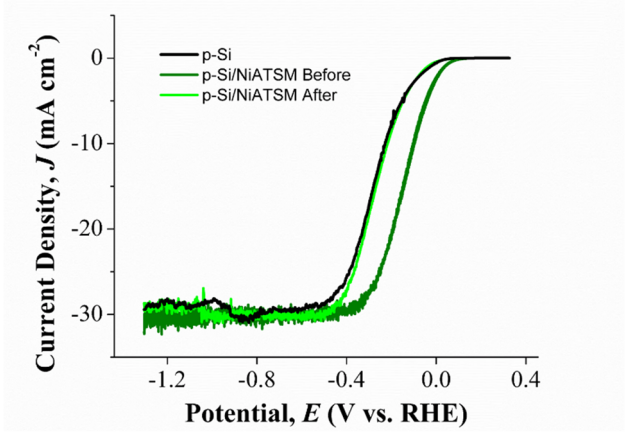

Fig. S3. Current density vs. potential (*J-E*) behavior of p-Si/NiATSM without Nafion in 1 M H_2SO_4 under 1 Sun AM1.5 illumination. The Before data is the initial, as-deposited performance and the After data is the performance after 1 h at -0.2 V vs. RHE.

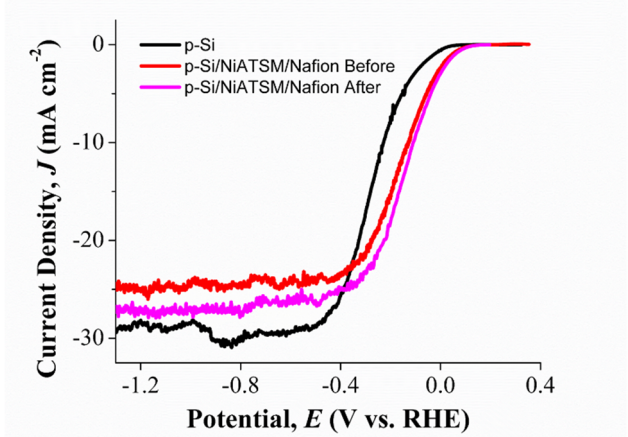

Fig. S4. Current density vs. potential (*J-E*) behavior of p-Si/NiATSM with Nafion in 1 M H_2SO_4 under 1 Sun AM1.5 illumination. The Before data is the initial, as-deposited performance and the After data is the performance after 1 h at -0.2 V vs. RHE.

operation (Fig. S3). After 1 hour of potentiostatic operation at -0.2 V vs. RHE, the photoelectrode *J-E* behavior became indistinguishable from that of bare p-Si. This performance decline was attributed to gradual detachment of the NiATSM catalyst from interfacial agitation during H_2 bubble formation. Thus, a Nafion solution was added to the NiATSM solution to provide an acid-compatible binding layer during drop-casting. The resulting current density vs. potential photoelectrochemical behavior for p-Si/NiATSM/Nafion photoelectrodes became much more stable (Fig. 3, Fig. S4). The photocurrent response slightly increased after the 1 hour potentiostatic measurement, which may be partially attributable to the beneficial effect of NiATSM molecular catalyst morphology stacking and restructuring as reported in our previous work.[5]

Effect of Nafion on the p-Si Performance

The NiATSM was cast from a dilute solution of Nafion (see Experimental Methods), with the cation-exchange selective ionomer used to enhance the binding of the molecular compound to the semiconductor surface while permitting stable performance in acidic media. As shown in Fig. S5, an equivalent thickness of Nafion film on p-Si in the absence of NiATSM had only a minor effect on the illuminated current density vs. potential behavior. There was a slight positive shift in potential for a Nafion film relative to a bare p-Si photoelectrode. This minor effect could speculatively be attributed to the charged groups in the Nafion sulfonic acid side chains creating a slight dipole at the interface, which contributes to band bending and has been experimentally demonstrated to affect the photoelectrochemical photovoltage.[6] However, initial *J-E* performance curves for p-Si/NiATSM with and without Nafion binder were indistinguishable between multiple electrodes within experimental error (Fig. 2).

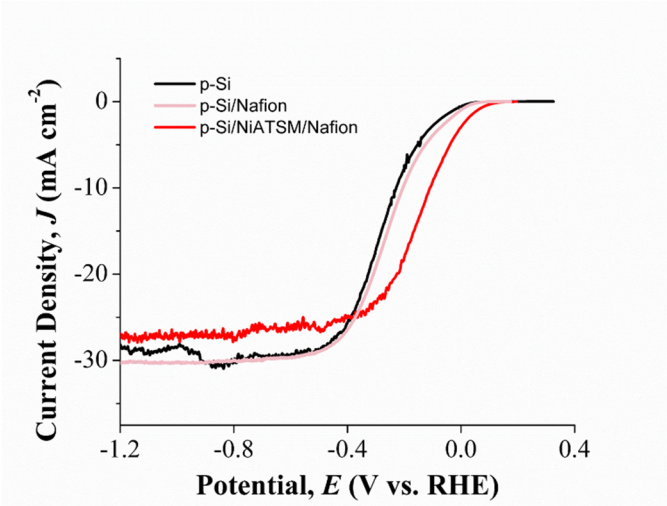

Fig. S5. Current density vs. potential (*J-E*) behavior in 1 M H_2SO_4 under 1 Sun AM1.5 illumination for bare p-Si, p-Si/Nafion, and p-Si/NiATSM/Nafion.

Elemental Mapping of NiATSM on p-Si

Following extended potentiostatic operation of the p-Si/NiATSM/Nafion photocathodes, the catalyst particles were observed to agglomerate into larger rodlike particle structures (Fig. 3). Energy dispersive x-ray spectroscopy (EDS) analysis was performed to map the distribution of the key elements before and after this restructuring. As seen in Fig. S6 below, Ni and S, which are primarily present in the NiATSM (S is a minor component in Nafion), are mostly confined to the observed particles even after the agglomeration. Fluorine, F, which is introduced in the polytetrafluoroethylene backbone of the Nafion binder, is initially observed to be uniformly distributed. However, after particle agglomeration, it was observed to be more concentrated along the edges of the rodlike NiATSM particle. Si, as the underlying substrate, displayed a strong signal everywhere, which was only weakened in the locations of the catalyst particle.

XPS of NiATSM and Nafion on p-Si

Although XPS data for NiATSM after cathodic cycling on glassy carbon substrates in aqueous acidic electrolyte has already shown a steady Ni oxidation state in our previous work,[5] it was measured and reported again here on p-Si photoelectrodes and in the presence of the Nafion binder. For an as-deposited p-Si/NiATSM without Nafion, a p-Si/Nafion without NiATSM, and p-Si/NiATSM/Nafion before and after 1 h under 1 Sun at -0.2 V vs. RHE in 1 M H_2SO_4, the measured binding energies for the Ni

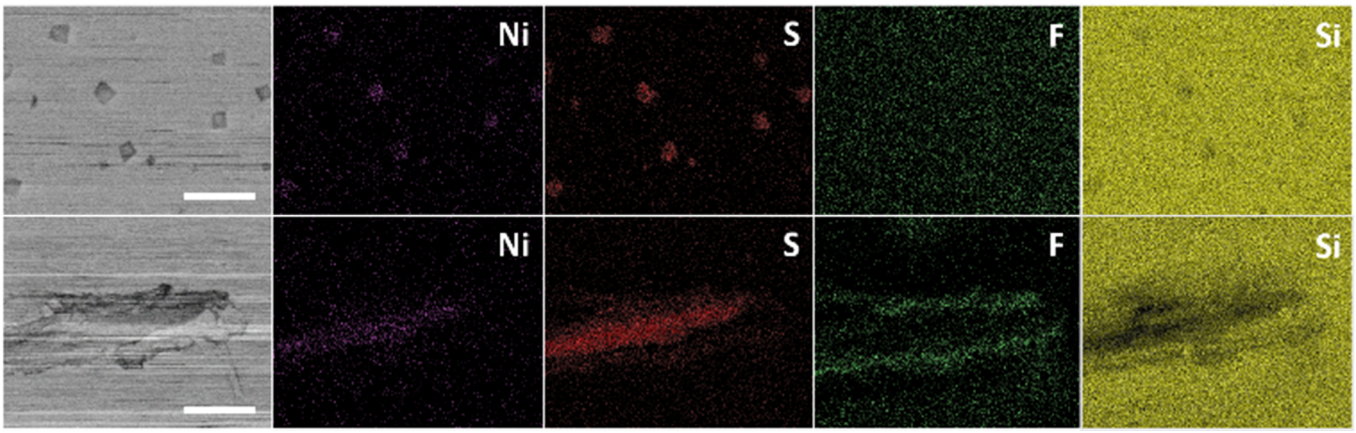

Fig. S6. SEM images (far left) and EDS corresponding elemental maps for Ni (purple), S (red), F (green) and Si (yellow) for p-Si/NiATSM/Nafion before (top panels) and after (bottom panels) 1 h at -0.2 V vs. RHE in 1 M H_2SO_4 under 1 Sun AM1.5 illumination. The scale bar is 20 µm.

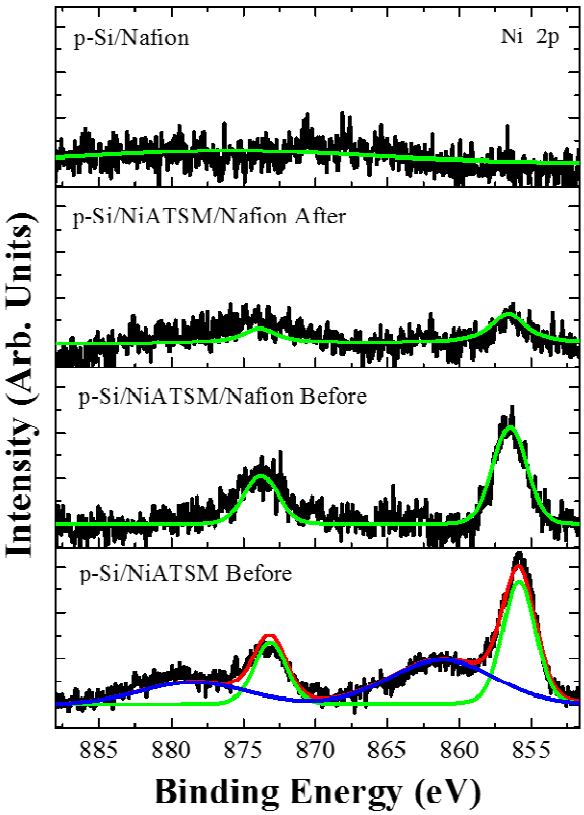

Fig. S7. XPS spectra for the Ni 2p region for various p-Si substrates. Before substrates were measured with as-deposited catalyst, and the After substrate had been exposed to 1 Sun at -0.2 V vs. RHE in 1 M H_2SO_4 for 1 h.

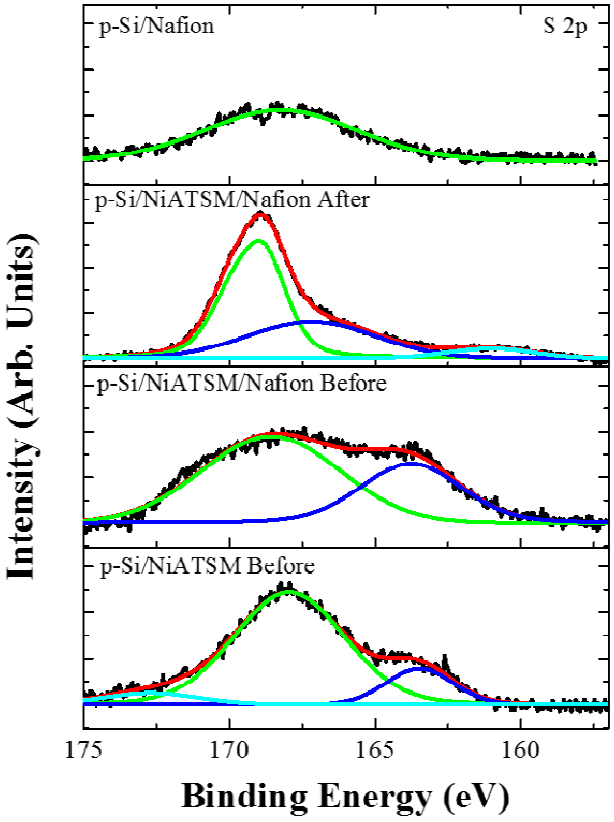

Fig. S8. XPS spectra for the S 2p region for various p-Si substrates. Before substrates were measured with as-deposited catalyst, and the After substrate had been exposed to 1 Sun at -0.2 V vs. RHE in 1 M H_2SO_4 for 1 h.

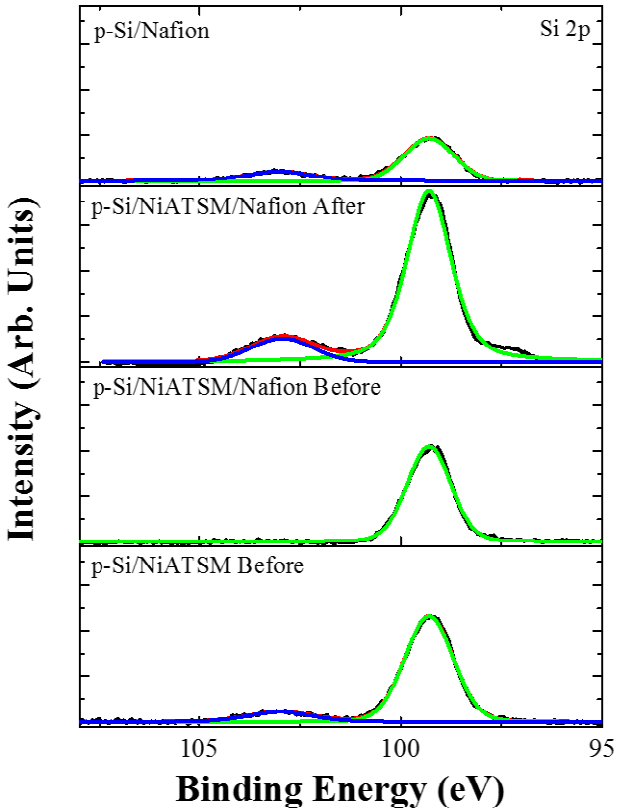

Fig. S9. XPS spectra for the Si 2p region for various p-Si substrates. Before substrates were measured with as-deposited catalyst, and the After substrate had been exposed to 1 Sun at -0.2 V vs. RHE in 1 M H_2SO_4 for 1 h.

2p, S 2p, and Si 2p regions are shown in Figs. S7, S8, and S9, respectively. Without Nafion, the as-deposited p-Si/NiATSM shows the same Ni 2p character as previously reported for NiATSM.[5] When the NiATSM is co-deposited with Nafion binder, the Ni 2p signal was significantly reduced in intensity, which is consistent with a thin surface coating of polymer reducing the signal (Fig. S7). The Ni 2p peak intensity was further reduced after operation, consistent with the dispersed catalyst particles concentrating into larger particles (Fig. 3) and leaving less area of exposed Ni to measure. However, the main Ni 2p peak position at ~856 eV remained unchanged before and after operation, indicating no shift in the oxidation state.

For sulfur, the XPS spectra is more complicated by the presence of the Nafion layer. Nafion polymer owes its cation-selective permeability to the negatively charged groups arising from the clustering of sulfonic acid side chains. Thus, there are S atoms present throughout the Nafion film, as evidenced by the broad S 2p peak observed for p-Si/Nafion without NiATSM catalyst (Fig. S8). For p-Si/NiATSM without Nafion, a sharper S 2p was observed at ~168 eV, which would be attributed to the Ni-adjacent S atoms in NiATSM (Fig. 1). When NiATSM is co-deposited with Nafion, the resulting S 2p spectra appears to be a convolution of the broad Nafion S peak and the underlying NiATSM S signal. Interestingly, after the p-Si/NiATSM/Nafion stability measurement, the sharper NiATSM S 2p peak increased in intensity relative to the spectra before photocathodic hydrogen evolution. The nature of this shift is not entirely clear, but we speculate that the NiATSM agglomeration to large

rodlike particles during operation leaves more of the NiATSM directly exposed to the x-ray signal, as opposed to the smaller as-deposited NiATSM clusters which have a surface coating of Nafion to interfere with the measurement.

The effect on the underlying Si substrate was also probed with the Si 2p XPS binding energy spectra (Fig. S9). After the 1 h stability measurement, the Si peak at 99.6 eV and the SiO_2 peak at 103.4 eV both became more intense relative to the as-deposited substrates. As observed in our SEM measurements after extended potentiostatic operation, the initial smaller microparticles of NiASTM left behind gaps in the Nafion thin film when they migrated and agglomerated into larger particles. We thus attribute the increased Si peak (and Si oxidation) to the underlying Si in these gaps being directly exposed to the x-ray.

Behavior of Electrodeposited Ni on p-Si

Metallic Ni was deposited photoelectrochemically on p-Si (see Experimental Methods) for comparison to the performance of photocathodes catalyzed with molecular NiATSM. By controlling the charge passed per electrode area during electrodeposition, well-controlled Ni loadings were achieved. With a single Ni site per NiATSM molecule, a molar loading of Ni of ~60 nmol cm^{-2} was present as NiATSM catalyst during photoelectrochemical measurements. Thus, 60 nmol cm^{-2} of electrodeposited Ni catalyst was used to directly compare the activity of an equivalent amount of metallic Ni. As shown in Fig. S10, this low loading of Ni as HER catalyst produced little improvement in the *J-E* behavior of a p-Si photocathode. Progressively higher loadings of Ni managed to reduce the overpotential, with a loading of 430 nmol cm^{-2} reaching 10 mA cm^{-2} at -0.080 V vs. RHE. This potential is comparable to that achieved for p-Si/NiATSM/Nafion photoelectrodes (Table 1), however, it required 7.2x as much Ni. Moreover, parasitic light absorption in the catalyst layer became more significant at this loading, leading to a 35% decrease in the light-limited current density.

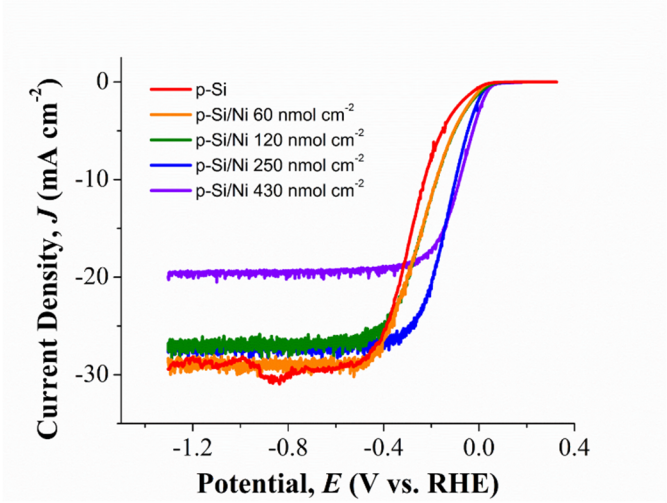

Fig. S10. Current density vs. potential (*J-E*) behavior of electrodeposited Ni/p-Si electrodes in 1 M H_2SO_4 under 1 Sun AM1.5 illumination as a function of Ni catalyst loading.

Behavior of NiATSM on Buried Junction n^+p-Si

Buried junction photocathodes were fabricated by producing a solid-state diode with an n^+ emitter layer. This approach can lead to better junction performance, and was shown in Fig. 4 to highlight the increased HER performance possible for Si/NiATSM photocathodes with this additional processing step. The *J-E* performance for a bare n^+p-Si photocathode is shown in Fig. S11 for comparison to the NiATSM-catalyzed behavior. At 10 mA cm^{-2}, the bare n^+p-Si had a potential of -0.110 V vs. RHE. Thus, the n^+p-Si/NiATSM/Nafion potential was shifted 135 mV positive relative to the uncatalyzed electrode, which was consistent with the behavior for p-Si electrodes without a buried junction (Table 1). The NiATSM with Nafion binder was also observed to be stable on buried junction n+p-Si photoelectrodes under the same operating conditions tested in Fig. 3a. At -0.2 V vs. RHE for 1 h, the current density stabilized at ~ 27 mA cm^{-2} (Fig. S12), consistent with the corresponding observed value during cyclic voltammetry.

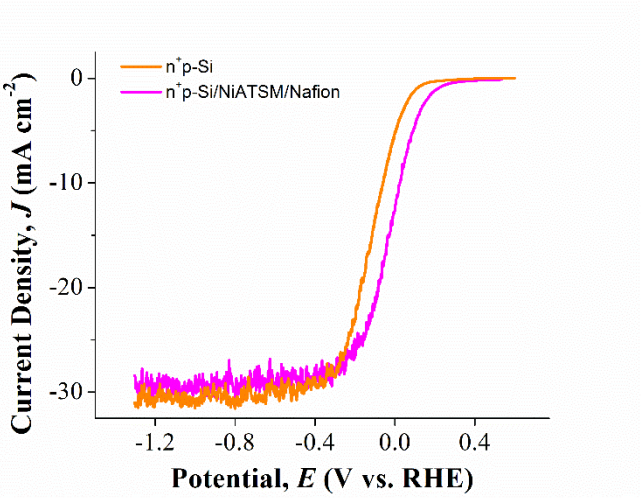

Fig. S11. Current density vs. potential (*J-E*) behavior in 1 M H_2SO_4 under 1 Sun AM1.5 illumination for bare n^+p-Si, and n^+p-Si/NiATSM/Nafion.

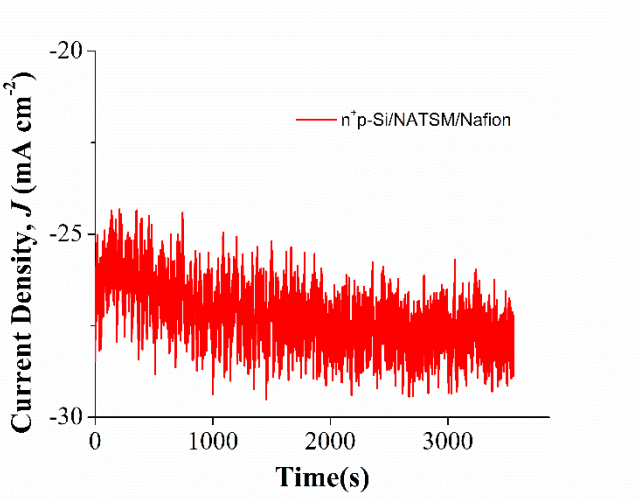

Fig. S12. Current density vs. time at -0.2 V vs. RHE under 1 Sun AM1.5 illumination in 1 M H_2SO_4 for n^+p-Si/NiATSM/Nafion.

References

1. P. J. Blower, T. C. Castle, A. R. Cowley, J. R. Dilworth, P. S. Donnelly, E. Labisbal, F. E. Sowrey, S. J. Teat and M. J. Went, *Dalton Trans.*, 2003, 4416-4425.
2. H. M. Betts, P. J. Barnard, S. R. Bayly, J. R. Dilworth, A. D. Gee and J. P. Holland, *Angew. Chem.-Int. Edit.*, 2008, **47**, 8416-8419.
3. I. Lombardi, S. Marchionna, G. Zangari and S. Pizzini, *Langmuir*, 2007, **23**, 12413-12420.
4. S. W. Boettcher, E. L. Warren, M. C. Putnam, E. A. Santori, D. Turner-Evans, M. D. Kelzenberg, M. G. Walter, J. R. McKone, B. S. Brunschwig, H. A. Atwater and N. S. Lewis, *J. Am. Chem. Soc.*, 2011, **133**, 1216-1219.
5. A. J. Gupta, N. S. Vishnosky, O. Hietsoi, Y. Losovyj, J. Strain, J. Spurgeon, M. S. Mashuta, R. Jain, R. M. Buchanan, G. Gupta and C. A. Grapperhaus, *Inorg. Chem.*, 2019, Submitted.
6. D. C. Gleason-Rohrer, B. S. Brunschwig and N. S. Lewis, *J. Phys. Chem. C*, 2013, **117**, 18031-18042.